Optimization of Electrically Conductive Films: Poly(3-methylthiophene) or Polypyrrole in Kapton

MARY ANN B. MEADOR,[1] DENISE HARDY-GREEN,[1,*] JUDITH V. AUPING,[1] JAMES R. GAIER,[1] LESLEY ANN FERRARA,[1,†] DEMETRIOS S. PAPADOPOULOS,[1,‡] JAMES W. SMITH[1,§] DENNIS J. KELLER[2]

[1]NASA Lewis Research Center, Cleveland, Ohio 44135; [2]RealWorld Quality Systems, Inc., Rocky River, Ohio 44116

Received 18 March 1996; accepted 22 April 1996

ABSTRACT: A method to generate conductive films composed of small amounts of conductive polymer absorbed into the surface of polyimide films has been optimized. Both pyrrole (PY) and 3-methylthiophene (3MT) were evaluated as precursors for the conductive phase. Predictive models were empirically derived for each precursor to describe the effects of polymerization variables on the conductivity of the films. The variables studied were found to be highly synergistic. An optimum set of conditions was found for each conductive polymer that produces the highest conductivity. Using *p*-3MT as the conductive phase, films with conductivity as high as 5.7 Ω^{-1} cm^{-1} can be produced, an improvement of four orders of magnitude over previously reported results with Kapton as a base polymer. The highest conductivity achieved using *p*-PY as the conductive phase was 0.041 Ω^{-1} cm^{-1}, still a two order of magnitude improvement over previously reported results. Mean mechanical properties of the 3MT-treated films were not significantly lower than that for untreated Kapton. The conductivities of *p*-3MT/Kapton films tested over time under ambient temperature in air persist fairly well for 300 days. © 1997 John Wiley & Sons, Inc. J Appl Polym Sci **63:** 821–834, 1997

Key words: conductive polymers; polythiophene; polypyrrole; statistical design of experiments

INTRODUCTION

Recently, composite films were reported that combine a conducting polymer with a flexible, insulating resin such as poly(ethylene terephthalate),[1] poly(methyl methacrylate),[2,3] polyethylene,[4] polystyrene,[5,6] or polyimide.[7,8] In all these instances, the films were prepared by infiltrating an insulating polymer with the precursor to a conductive polymer and oxidatively polymerizing *in situ.* The resulting electrically conductive composite films contain only small amounts of the conductive polymer and, hence, retain some of the properties of the base polymer.

Examples of the highest conductive hybrid films produced within the previously referenced studies are summarized in Table I, including oxidation conditions used and resulting conductivity in Ω^{-1} cm^{-1}. The highest conductivities were achieved with polythiophene in polystyrene.[6] The best results using polypyrrole as a conductive polymer were also obtained with polystyrene[5] as a base polymer, but the films produced were an order of magnitude less conductive than with the films containing polythiophene.

The best composite films using a polyimide[7,8] as a base polymer were three or four orders of magnitude less conductive than were the polystyrene films. The authors suggested that this is be-

Correspondence to: M. B. Meador.
* Resident research associate from the University of Akron, Akron, OH, 44325.
† NASA OAI Summer Intern.
‡ Resident research associate from Case Western Reserve University, Cleveland, OH 44135.
§ Resident research associate from Cleveland State University, Cleveland, OH 44135.

Table I Summary of Results Achieved from Monomer Infiltration Followed by Oxidative Polymerization (from Literature References)

Polymer		Best Oxidation Conditions			Conductivity (Ω^{-1} cm^{-1})
Insulating Base	Conductive	Oxidant	Temperature	Time	
Kapton[7]	Polypyrrole	0.75*M* $FeCl_3$ in H_2O	Ambient	5 min	4×10^{-4}
Soluble polyimide[8]	Polypyrrole	0.62*M* $FeCl_3$ in H_2O	Ambient	16 h	6×10^{-4}
Poly(etheylene terephthalate)[1]	Polypyrrole	0.62*M* $FeCl_3$ in H_2O	0–10°C	5–10 h	0.03 to 0.1
Polystyrene[5]	Polypyrrole	1.2*M* $FeCl_3$ in methanol	Ambient	2 h	0.49
Polystyrene[6]	Polythiophene	1.2*M* $Fe(ClO_4)_3 \cdot 6H_2O$ in acetonitrile	Ambient	10 min	4.5

cause polyimides are not as porous or would be unable to swell sufficiently for infiltration of monomer as in the other previously referenced work. It is not clear, however, whether the lower conductivities obtained using polyimides could have been merely the result of differing oxidation conditions. In both polyimide studies, lower oxidant concentrations were used relative to the polystyrene studies. With poly(ethylene terephthalate) and polypyrrole,[1] the same concentration of oxidant was used as in the polyimide examples and a much higher conductivity was obtained; however, the oxidation was carried out at a lower temperature. Oxidation times also varied widely between studies (from 5 min to 16 h) with a seemingly minimal effect on resulting conductivity. Hence, it is tenuous at best to draw conclusions about the effect of a base polymer (and oxidation conditions) on the conductivity of the hybrid films.

Chemical polymerization of pyrrole with various oxidants has been known since 1916,[9] although in recent years, electrochemical polymerization has been more thoroughly investigated.[10] Recent studies of chemical polymerization[11–13] show that variables such as time, temperature, and oxidant concentration have a strong effect on the conductivity of the polypyrrole produced. Chemically induced oxidative polymerization of thiophenes is also known.[10,14]

We are interested in developing hybrid polymeric materials that combine high electrical conductivity with long-term environmental stability, good processability, and good mechanical properties. Of primary importance are electrically conductive composite films made from polyimides and other engineering resins. If conductivities as high as those obtained with polystyrene could be achieved with polyimides, such materials would have utility in many aerospace applications where a combination of properties is needed. Use of polymers in applications such as electromagnetic interference (EMI) shielding enclosures, spacecraft grounding, charge dissipation, and antenna reflector surfaces would result in tremendous weight savings over the metals currently used.[15]

The approach of infiltration by a conductive polymer precursor followed by *in situ* oxidative polymerization is particularly attractive because the conductive phase is added after the base polymer is completely cured. There are many examples of blending conductive polymers with soluble or uncured insulating resins to make hybrid materials.[10,16] Unfortunately, polyimides and other such polymers are often insoluble when fully cured and the conductive polymer would not survive the cure conditions. The infiltration technique is also amenable to large-scale processing. In addition, it has possible utility as a surface treatment for a polymer structure without detrimentally affecting other bulk properties throughout the structure.

In this article, we discuss the optimization of the conductivity of polyimide-based composite films. The study was carried out by examining the effect of several processing parameters on the ultimate conductivity and mechanical strength of the films. The polyimide base chosen for this study was Kapton® (DuPont) since it is readily available commercially in film form. In addition, we

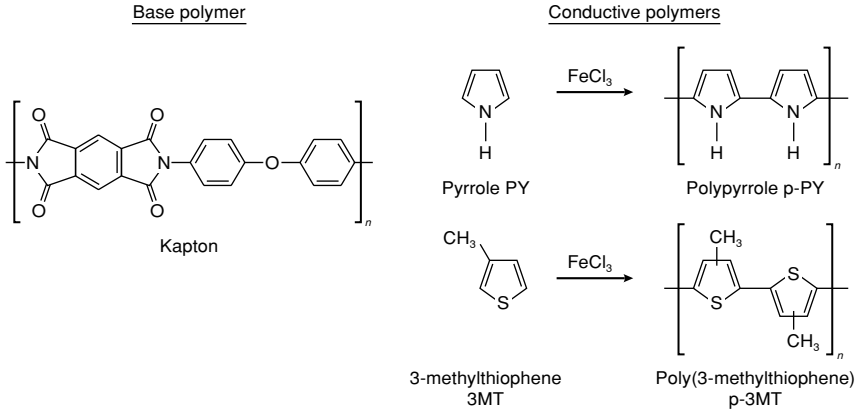

Scheme 1.

chose to examine the effect of two monomers for infiltration, pyrrole (PY) vs. 3-methylthiophene (3MT), for the conductive phase of the composite films, as shown in Scheme 1.

PY was chosen for this investigation because it has been studied extensively as a starting material for this technique. However, as previously discussed, the effect of the oxidation variables and the synergistic effects among variables on the conductivity of polypyrrole hybrid films are not well understood. 3MT was chosen because it has similar handling characteristics to PY (a liquid at room temperature with a similar boiling point). In addition, as shown in the previous studies,[5,6] the resulting conductivities may be higher with polythiophenes. Furthermore, polyalkylthiophenes have been shown to be more stable to air and moisture than are polypyrroles.[17]

We identified five processing variables in making these composite films. These were exposure time and temperature for the monomer infiltration and time, temperature, and oxidant concentration for the *in situ* oxidation. Statistically designed experiments were used to examine the effects of these variables and interactions among variables on the electrical conductivity and mechanical strength of the films for each monomer. The morphology of the hybrid films was also characterized by scanning electron microscopy (SEM). In addition, as a gauge of stability, the conductivity of samples was measured as a function of aging time under various conditions.

EXPERIMENTAL

Pyrrole (PY; 98%) and 3-methylthiophene (3-MT; 99+%) were purchased from Aldrich Chemical Co. and distilled before use. Since the monomers could be reused between infiltration runs, purity was also monitored throughout the study using a Hewlett-Packard 5890 gas chromatograph (GC), and monomers were redistilled as necessary. Anhydrous $FeCl_3$ was also obtained from Aldrich and used as received. Acetone and acetonitrile (HPLC grade) were supplied by J. T. Baker. The acetonitrile was stored over activated 4 Å molecular sieves for a minimum of 24 h prior to use.

The substrate or host polymer used in all experiments was Kapton, a condensation polyimide film. Kapton is the DuPont trade name for poly(*N,N′*-[*p,p′*-oxydiphenylene]pyromellitimide). Kapton is synthesized from the stoichiometric addition of 1,2,4,5-benzenetetracarboxylic dianhydride and 4,4′-diaminophenyl ether in a suitable solvent. This reaction produces an intermediate polyamic acid solution that can be cast into film and thermally cured to the polyimide via cyclodehydration. The Kapton used in all of the experiments was obtained as a fully cured film from Electrolock in 24 in. (61.92 cm)-wide rolls, nominally 0.005 cm in thickness. Kapton film specimens were cut with a rotary blade into 7 × 2.5 cm specimens and randomly chosen for each experiment. Moisture retention can be a problem with Kapton films. Reported data indicate that water absorption up to 2% by weight is not uncommon. Hence, the film samples were dried at 50°C under vacuum for at least 12 h prior to the monomer soak cycle.

Typical Film Soak Procedure

Five film specimens were placed in a 250 mL round-bottomed flask. Either neat PY or 3MT

(150 mL) was added to the flask. This volume was sufficient to keep all exposed film surfaces immersed. The films were agitated (either by mechanical stirring or wrist-action shaker) in the monomer for a specified time under nitrogen. In an initial study to identify conditions that would yield maximum absorption of the monomer, the soak time was varied between 24 and 72 h. The soak temperature was varied between ambient and reflux. Soaking for greater than 24 h at any temperature was found to have no effect on the amount of monomer absorbed. Hence, for the rest of the experimental runs, soaks were carried out at room temperature for 24 h. After soaking, the film specimens were rinsed with acetone and blotted dry. The films were further dried under flowing nitrogen for approximately 1 min. The samples were weighed before and after soaking to estimate the amount of monomer absorbed. Monomer uptake (95% confidence) was 11–14 wt % for PY and 8–11 wt % for 3MT.

Oxidative Polymerization

Oxidative polymerization immediately followed the monomer soak. Anhydrous ferric chloride was dissolved in dry acetonitrile to make solutions of various concentrations, ranging from 0.4 to 4.0*M,* according to the experimental design. The oxidant solution (150 mL) was poured into a 250 mL round-bottomed flask fitted with a nitrogen port and allowed to equilibrate at the oxidation temperature under nitrogen and agitation. The oxidation temperature, which ranged from −10 to 70°C, was controlled using a recirculating bath. The film specimens were added to the solution and oxidized for 0.5–8 h at the set temperature, according to the design. When the oxidation time expired, the films were removed from the reddish brown oxidant solution. The five specimens were separately rinsed with portions of fresh, dry acetonitrile until the rinse solution was colorless. The films were blotted dry with filter paper and air-dried for 1 h. Dog bone-shaped specimens (ASTM type V) were cut from each of the five films and reserved for tensile tests. Specimens for conductivity measurement (nominally 1.5 × 20 mm) were cut from the remaining scraps.

Untreated Kapton films are amber in color. After infiltration and oxidative polymerization, the films darken considerably. Initial conductivity measurements were made within 24 h of the experiment completion. Specimens that resulted in the highest electrical conductivity measurements were black and completely opaque.

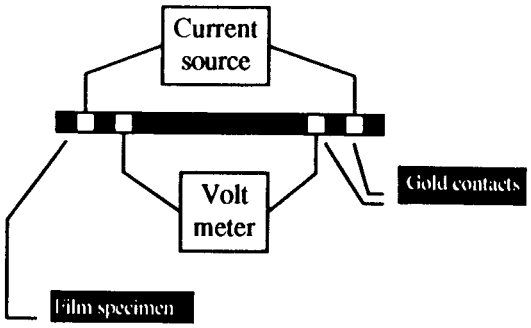

Figure 1 Standard four-point conductivity test schematic.

Conductivity Measurements

A standard four-point measurement technique was used to test the conductivity for all of the film specimens (Fig. 1). Four in-line gold contacts were sputtered onto the conductivity specimens. A current, I, was applied across the two outer contacts with a Keithley 225 DC current source. The voltage drop, V, was measured with a Keithley 181 nanovoltmeter at three current levels between 1 and 500 μamps. Plots of I vs. V were linear for all samples. The conductivity, σ, in Ω^{-1} cm^{-1}, was calculated according to the following equation: $\sigma = Il/twV$, where w = width, l = length, and t = thickness. The thickness of the conductive layer probably varies with the oxidation conditions. For simplicity in the calculation, we used t = 0.005 cm, the thickness of the entire film. This calculation, which gives conductivity as a bulk property, probably results in a lower value than actually exists in the surface layer.

Tensile Tests

Tensile tests were performed on treated and untreated Kapton ASTM Type V dog bones at ambient temperature and humidity.[18] Five dog bone specimens of each of the treated films and 10 specimens of untreated Kapton were tested in all. The tests were conducted on a Model 4505 load frame made by Instron with Series IX software. The crosshead speed was 0.2 in. per min and the data acquisition rate was 10 points per s. The maximum load was recorded, and maximum mechanical stress and load-to-width ratios at maximum load were calculated. The specimens were of insuf-

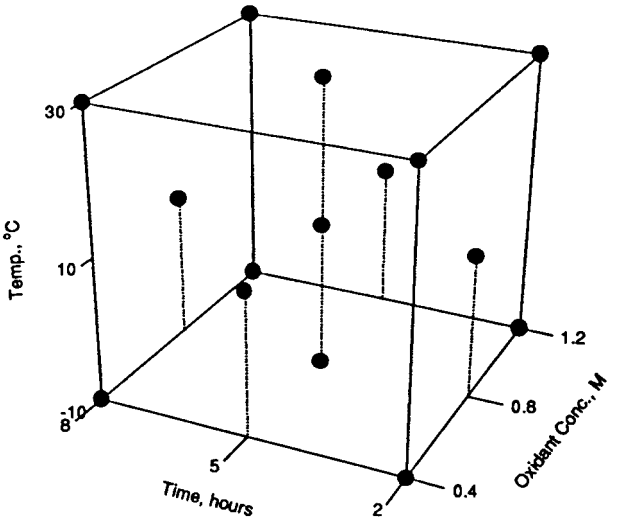

Figure 2 Plot of all experimental runs of face-centered central composite design.

ficient length to obtain modulus and maximum strain values.

Scanning Electron Microscopy

SEM was performed on selected treated and untreated Kapton film specimens. Studies included the examination of the surfaces and film cross sections. No microtome was available for proper cross sectioning. Several alternative techniques were attempted to characterize the degree of subsurface oxidation, including liquid N_2 fracture and simple scalpel cuts along a straight edge. The thinness of the films precluded clean fractures in liquid N_2. The films separated by a mixed fracture and tear mechanism. The relatively planer scalpel cuts provided a more suitable surface for chemical characterization. Approximately 50 Å of palladium was sputtered on all samples to ensure conductivity in the electron beam. Secondary (SE) and backscattered (BSE) electron images were obtained on selected areas of each sample.

RESULTS AND DISCUSSION

The oxidative polymerization process was examined for the effects of time, temperature, and oxidant concentration on the conductivity and strength of the final films. To minimize the number of experiments in the study, we used a face-centered central composite experimental design. Three levels of time (2, 5, and 8 h), three levels of temperature (−10, 10, and 30°C), and three concentrations of $FeCl_3$ in acetonitrile (0.4, 0.8, and 1.2M) were investigated. The scope of the design can be described as a box with each of the three axes representing one of the three variables (as shown in Fig. 2). The experimental conditions run in this type of design include all eight corners of the box, the center of each of the six faces, and the center of the box for a total of 15 different experiments. This allows for statistical analysis of the responses (conductivity and strength) in terms of time, temperature, and concentration using a full quadratic model, including all two-way interactions among variables. In addition, four repeats of the center of the box were run to quantify experimental reproducibility. Thus, a total of 19 experiments was carried out for each monomer. From this, the significance of effects as well as model adequacy and reliability can be judged. The 19 experiments for each monomer were carried out in a randomized run order. Two sets of five Kapton films, one set in PY and one set in 3MT, were soaked for 24 h at room temperature with stirring. The monomer-treated films were then oxidized in pairs, in the run order and under the conditions described in Table II.

The treated films all tended to be flexible and uniformly dark in appearance after oxidation. Electrical conductivity was measured at each oxidation condition for each monomer. These values are given in Table II. Maximum mechanical stress at maximum load was measured for all the films by the tensile test. Because tensile tests are flaw-sensitive, five samples from each batch at each experimental condition were measured. The values given in Table II and used for analysis are the median values for each set of five films.

Both the p-PY and p-3MT conductivity values are plotted vs. experimental run order in Figure 3. Even without further analysis, this plot dramatically shows that 3MT-treated films have higher conductivity than that of PY-treated films, since nearly all the p-3MT/Kapton data are higher than nearly all the p-PY/Kapton data. A simple paired t-test on the mean log conductivities confirms that 3MT-treated Kapton is significantly more conductive (>99.99% confidence) than is the PY-treated Kapton, across all oxidation conditions.

A plot of maximum stress from tensile tests vs. run number of both p-3MT/Kapton and p-PY/Kapton films is shown in Figure 4. For untreated Kapton, the mean value for maximum stress calculated from tensile tests on each of 10 specimens

Table II Oxidation Conditions and Conductivity Data for PY- and 3MT-treated Films

Experimental Conditions				*p*-PY/Kapton		*p*-3MT/Kapton	
Run Order	$FeCl_3$ Concn (*M*)	Time (h)	Temp (°C)	Conductivity (Ω^{-1} cm^{-1})	Maximum Stress (psi)	Conductivity (Ω^{-1} cm^{-1})	Maximum Stress (psi)
1	1.2	2	−10	9.10×10^{-3}	24,490	8.55×10^{-3}	32,245
2	0.4	5	10	2.14×10^{-2}	39,070	8.42×10^{-2}	33,340
3	0.8	5	10	6.02×10^{-3}	40,840	1.87×10^{-1}	48,130
4	0.8	2	10	1.99×10^{-2}	35,480	2.23×10^{-1}	35,920
5	0.4	8	30	3.28×10^{-3}	11,450	2.33×10^{-1}	25,370
6	0.4	2	−10	3.06×10^{-4}	31,010	1.12×10^{-2}	28,740
7	0.8	5	−10	1.51×10^{-4}	27,120	2.38×10^{-2}	31,090
8	1.2	2	30	7.42×10^{-3}	23,090	7.30×10^{-1}	28,120
9	1.2	8	−10	3.05×10^{-4}	31,400	2.08×10^{-1}	32,920
10	1.2	5	10	5.35×10^{-4}	30,240	2.44×10^{-1}	33,770
11	0.8	5	30	2.21×10^{-3}	20,470	1.09×10^{0}	28,770
12	0.4	2	30	2.71×10^{-3}	21,530	6.46×10^{-1}	32,770
13	0.8	5	10	6.56×10^{-4}	32,790	2.77×10^{-2}	38,420
14	0.4	8	−10	2.97×10^{-4}	34,010	2.18×10^{-1}	35,840
15	0.8	5	10	7.91×10^{-3}	30,870	2.97×10^{-1}	30,620
16	0.8	5	10	1.43×10^{-3}	28,810	2.03×10^{-1}	33,350
17	0.8	8	10	2.80×10^{-3}	29,040	9.25×10^{-1}	33,830
18	1.2	8	30	1.95×10^{-3}	25,760	8.36×10^{0}	29,510
19	0.8	5	10	4.74×10^{-3}	31,810	7.73×10^{-2}	34.680

is 34136 psi with a standard deviation of 3757 psi. The solid line in Figure 4 represents the mean value of untreated Kapton and the dotted lines are at ±2 standard deviations. Most of the data from the treated films falls within the dotted lines for untreated Kapton. An ANOVA (ANalysis Of VAriation) for comparing the mean maximum stress for each treatment type with untreated Kapton was performed. The comparison indicated no statistically significant difference between 3MT-treated and untreated films. For PY-treated

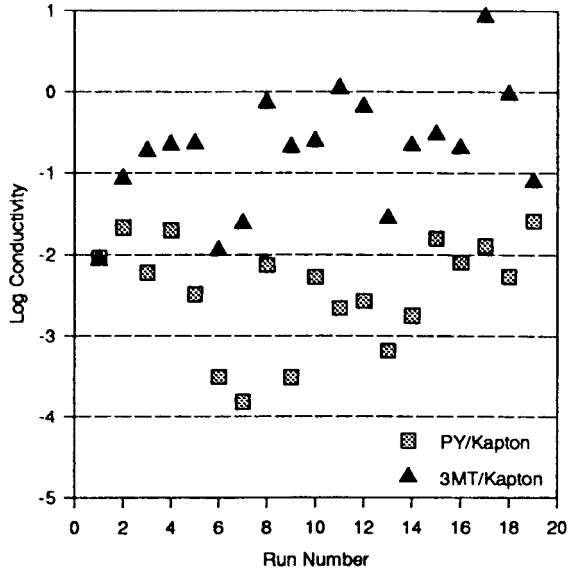

Figure 3 Plot of log conductivity vs. experimental run order.

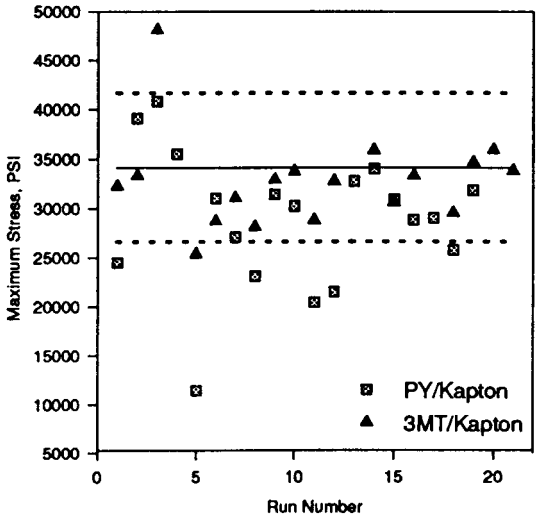

Figure 4 Plot of maximum stress vs. experimental run number. Solid line is mean value for untreated Kapton and dotted lines are ±2 standard deviations.

Table III Summary Statistics for Predictive Models

Data Set	Response	Model Terms (% Significance)	No. Experiments	Residual df	Standard Error of Estimate	R^2
p-PY/Kapton	Log conductivity	Temp (98.5) Time (96.1) Time × oxidant (91.6) $Temp^2$ (99.5) $Oxidant^2$ (92.5)	19	13	0.43 log Ω^{-1} cm^{-1}	0.68
p-3MT/Kapton	Log conductivity	Temp (98.5) Time (99.9) Oxidant (100) Time × temp (97.8) Time × oxidant (95.4) Temp × oxidant (92.5)	18[a]	11	0.27 log Ω^{-1} cm^{-1}	0.91
p-PY/Kapton	Maximum stress (tensile)	Temp (99.7) $Temp^2$ (99.9) Temp × oxidant (95.4)	19	15	4058 psi	0.71
p-3MT/Kapton	Maximum stress (tensile)	Temp (96.5) $Temp^2$ (99.7) Temp × time (95.6)	18[b]	14	2204 psi	0.62
p-3MT/Kapton (extended set of experiments)	Log conductivity	Temp (100) Time (99.6) Oxidant (97.8) Oxidant × temp (99.6) Time × temp × oxidant (95.0) $Temp^2$ (99.9) $Temp^3$ (98.0) $Oxidant^2$ (93.7) $Oxidant^2$ × temp (99.7)	41[a]	31	0.44 log Ω^{-1} cm^{-1}	0.75

[a] Run 13 dropped from analysis as experimental outlier.
[b] Run 3 dropped from the analysis as experimental outlier.

Kapton, mean maximum stress was only marginally significantly lower than that of untreated Kapton.

The values for the responses, conductivity, and maximum stress, obtained under different oxidation conditions for each of the films, were also analyzed by multiple linear least-squares regression. In this way, mathematical models describing the responses in terms of the oxidation conditions could be empirically derived. These response surface models can be used to predict the conductivity of films produced under conditions other than those measured experimentally.

PY- and 3MT-treated film data were analyzed separately. All independent variables were transformed to the −1 to 1 range prior to modeling to minimize correlation among terms. The conductivities were log-transformed for analysis. A 10-term full quadratic model of the form

$$\begin{aligned}\text{response} = {} & A + B\text{*TEMP} + C\text{*TIME} \\ & + D\text{*OXIDANT} + E\text{*TEMP}^2 + F\text{*TIME}^2 \\ & + \text{G*OXIDANT}^2 + H\text{*TEMP*TIME} \\ & + I\text{*TEMP*OXIDANT} + J\text{*TIME*OXIDANT}\end{aligned}$$

was entertained in each set of data. Terms not statistically significant (<90%) were dropped from the model by the stepwise modeling technique. Significant terms in the models and summary statistics are given in Table III.

The response surface models can be used to predict the conditions that produce optimum con-

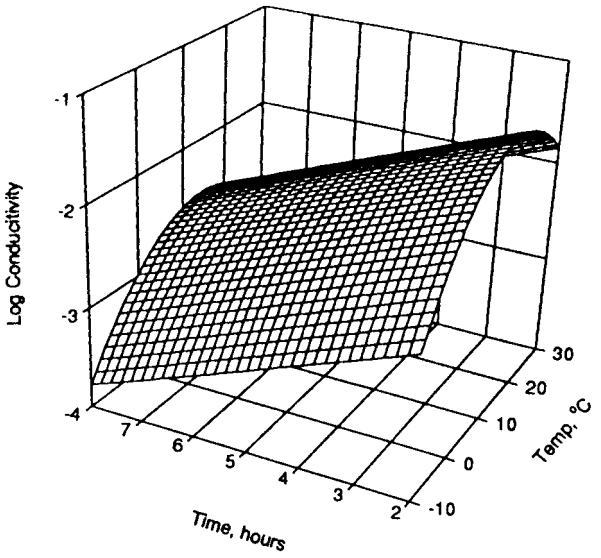

Figure 5 p-PY/Kapton surface with $FeCl_3$ concentration = 1.2M.

ductivity. For p-PY/Kapton films, the log conductivity is predicted by the model to be at a maximum when the monomer-soaked film is oxidized for 2.0 h at 17.6°C with 1.2M $FeCl_3$. Longer times and higher temperatures probably overoxidize the p-PY. Predicted conductivity for the optimum conditions is 0.041 Ω^{-1} cm^{-1}. An actual film treated under these conditions resulted in a measured conductivity value of 0.044 Ω^{-1} cm^{-1}, which is in excellent agreement with the predicted value. It may be possible to achieve higher conductivities by using methanol as the oxidation solvent as reported by Machida et al.[11] and Whang et al.[13]

The predicted conductivity response surface for PY-treated films, with oxidant concentration held constant at the optimum value of 1.2M, is shown in Figure 5. Temperature is shown to have a significant second-order effect on log conductivity, with an optimum conductivity predicted at 17.6°C for a 2 h oxidation. Also at 1.2M $FeCl_3$, time has a linear effect on log conductivity, with conductivity strongly decreasing with increasing time. There is no significant synergistic/interactive effect between time and temperature.

A response surface, with temperature held constant at its optimum value of 17.6°C, is shown in Figure 6. This plot reveals a strong interactive effect between oxidant concentration and time. In essence, at a low concentration of the oxidant, there is no detectable increase or decrease in log conductivity with respect to time. However, at high oxidant concentration, there is a strong increase in log conductivity with decreasing time. Although the oxidation solvents are not the same, this observation is in agreement with the literature results shown in Table I. The first two entries describe results where only oxidant concentrations less than 0.8M were used. The conductivities reported ranged from 4 to 6 $\times$ 10^{-4} Ω^{-1} cm^{-1} (or in log conductivity -3.4 to -3.2). This difference is not statistically significant, although the oxidant time ranged from 5 min to 16 h.

For p-3MT-containing films, an analysis of log conductivity using multiple linear regression gave the summary statistics shown in Table III. Reaction time, temperature, and oxidant concentration all have a significant linear effect on the log conductivity, and all three variables interact strongly with each other. Another statistically designed study of the polymerization of 3-octylthiophene was recently reported[19] where temperature did not have a significant effect on the polymerization. However, the temperature range studied in that design was only up to 10°C.

The maximum achievable conductivity within the design space is predicted to be 5.7 Ω^{-1} cm^{-1} by oxidizing the film for 8 h at 30°C in 1.2M $FeCl_3$. Actual experimental values obtained under these conditions resulted in a mean value of 5.0 Ω^{-1} cm^{-1} for three different runs, which is in good agreement with the prediction. The predicted conductivity response surface for p-3MT/Kapton, with oxidant concentration held constant at the optimum value of 1.2M, is shown in Figure 7.

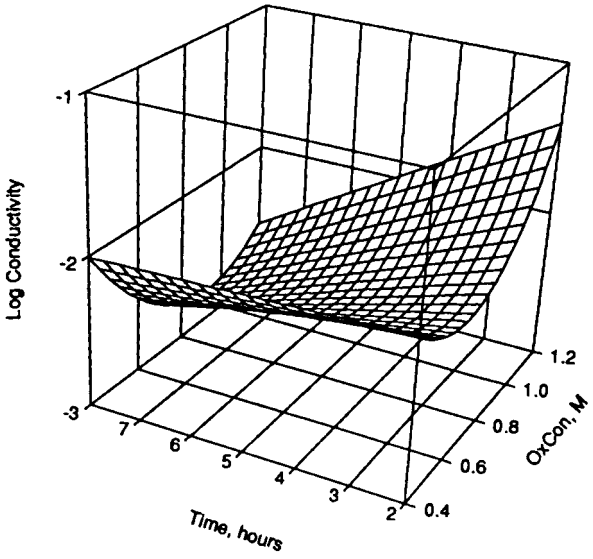

Figure 6 p-PY/Kapton surface with temperature = 17.6°C.

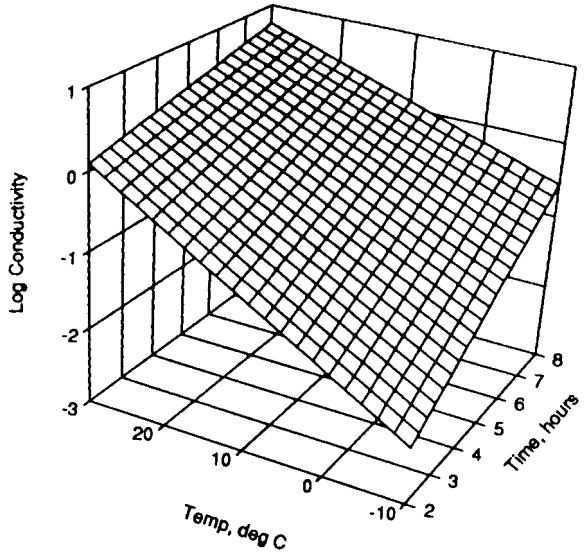

Figure 7 p-3MT/Kapton surface with oxidant concentration = 1.2M.

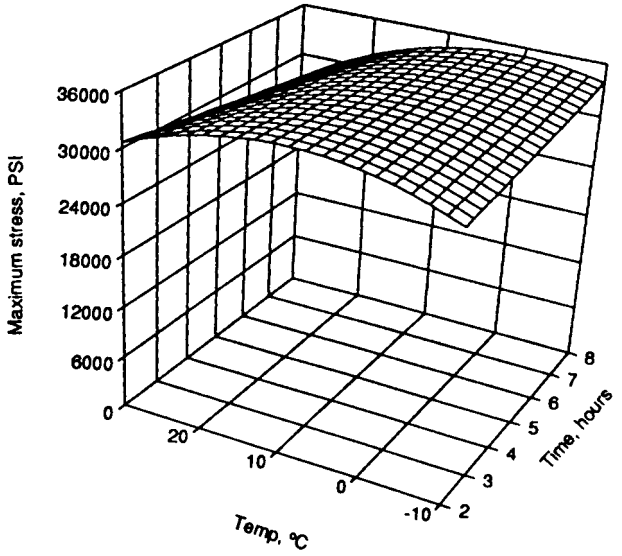

Figure 8 Response surface for p-3MT/Kapton maximum stress with oxidant concentration held constant at 1.2M.

Summary statistics for multiple linear regression analysis of maximum stress are also shown in Table III. The analysis reveals that for both polymers temperature has the strongest effect on maximum stress. Response surfaces of maximum stress vs. temperature and time with oxidant concentration held constant at 1.2M are shown in Figure 8 for p-3MT/Kapton and Figure 9 for p-PY/Kapton (graphed on the same z-scale). Although maximum stress decreases for both p-3MT and p-PY films with increasing temperature, the effect is much more pronounced with p-PY. However, at the oxidation conditions predicted to give the highest conductivity for p-PY, the mean maximum stress value is predicted to be 31,000 psi, which is not significantly different from the mean stress value measured for untreated Kapton. At the oxidation conditions predicted to give the highest conductivity for p-3MT, the mean maximum stress is predicted to be 27,000 psi, which is only marginally significantly lower than that measured for untreated Kapton. To obtain predicted mean maximum stress values not significantly different from untreated Kapton for p-3MT/Kapton, oxidation time can be limited to 2 h. For a 2 h oxidation, the optimal conditions of 30°C and 1.2M $FeCl_3$ still yield a predicted conductivity in excess of 1.5 Ω^{-1} cm^{-1} and a predicted mean maximum stress of 31,000 psi.

Since the optimum conductivity of p-3MT/Kapton is at one corner of the design space, it appeared that higher conductivities might be possible by going to longer reaction times, higher temperatures, and/or higher oxidant concentrations. To explore this prospect, additional experiments were run including oxidation conditions up to 70°C and 4M $FeCl_3$ concentration. It was not possible to increase oxidation time with the experimental setup. However, it was of interest to see what levels of conductivity could be obtained with shorter times. It would be preferred to be able to achieve the *same* optimum conductivities in *less*

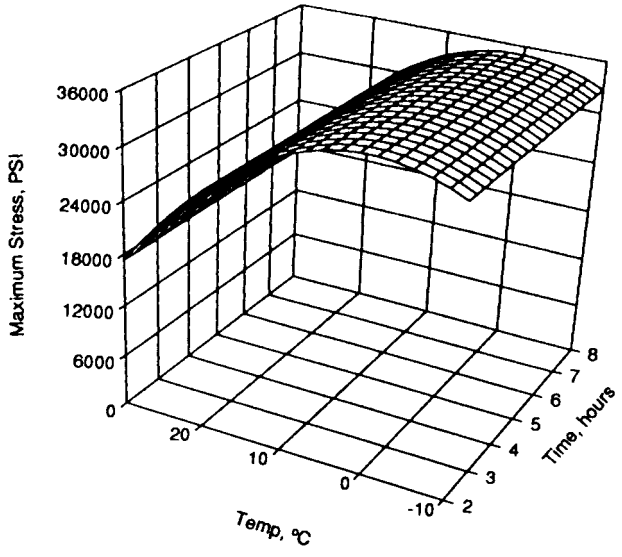

Figure 9 Response surface for p-PY/Kapton maximum stress with oxidant concentration held constant at 1.2M.

Table IV Additional Experimental Runs Using Oxidation Conditions Outside Original Design Space

Run No.	$FeCl_3$ Concentration (mol/L)	Time (h)	Temperature (°C)	Conductivity (Ω^{-1} cm^{-1})
23	1.2	2	30	1.78
26	4	0.5	70	0.554
27	1.2	0.5	70	1.53
30	1.2	4	30	1.70
31	4	4	30	0.662
32	1.2	0.5	30	0.184
33	4	0.5	30	7.54E-02
34	2.6	0.5	50	1.68
37	1.2	4	50	2.18
38	2.6	4	50	0.175
39	1.2	0.5	50	0.830
42	4	0.5	−10	0.174
43	4	8	−10	8.82E-02
45	0.4	0.5	70	2.22
48	4	2	50	7.19E-04
51	0.4	8	50	9.02E-02
52	0.4	8	30	3.02
53	1.2	8	30	1.35
54	4	8	30	0.192
55	0.4	8	30	5.29
56	1.2	8	30	5.19
57	4	8	30	0.118
58	2.85	4	18	0.465
59	2.85	0.5	18	8.05E-02
60	2	8	18	0.299
61	1.2	2	50	0.220

time with higher temperatures and/or higher oxidant concentrations. Hence, run times down to 0.5 h were also explored. Altogether, another 26 3MT experiments were run based on a sequential design strategy, including 20 experiments outside the original data space and six experiments around the original predicted optimum. The resulting conductivities are shown in Table IV.

Missing run numbers in Table IV represent experiments which gave unmeasurable conductivities (below 10^{-4} Ω^{-1} cm^{-1}). These consisted of runs of oxidation conditions at the extreme corners of the new design space. Runs at 50°C and higher temperatures in combination with the highest oxidant concentration as well as those at the lowest temperature and shortest time were all unmeasurable. At 70°C, only the 0.5 h experiments gave dark-colored films with measurable conductivities. Films oxidized for longer than 0.5 h at 70°C were the same amber color as that of untreated Kapton and were unmeasurable. For the three 0.5 h runs at 70°C, conductivity appears to decrease slightly with increasing oxidant concentration, but these runs were not used in the analysis.

The log conductivities from all of the 3MT experiments up to 50°C, including those from the first set of runs and the extended set, were combined for multiple linear regression analysis. The data could not be fit with a simple quadratic model. However, because all the experimental runs together contained at least four levels each, for all three variables, a 20-term cubic model could be entertained. As before, terms not statistically significant (<90%) were dropped from the model using the stepwise modeling technique. Significant terms in the model and summary statistics of the analysis are presented in Table III. The new predicted optimum of 5.6 Ω^{-1} cm^{-1} for oxidation at 38°C for 8 h and 2.0*M* oxidant concentration is just outside the original design space. However, it is not significantly different in conductivity than that predicted from the first set of experiments. The response surface with oxidant

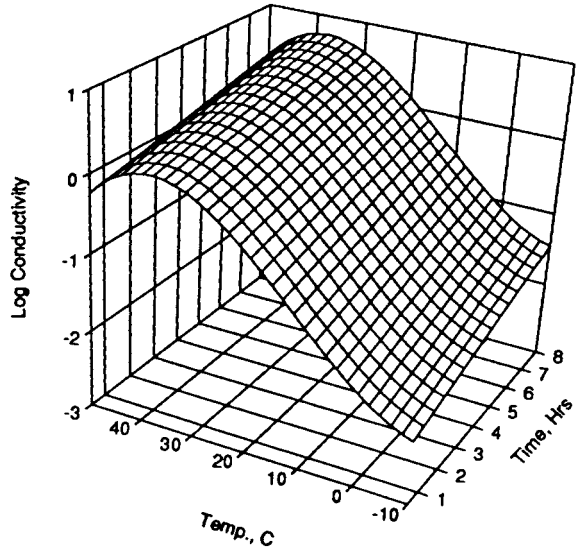

Figure 10 Response surface for *p*-3MT/Kapton with oxidant concentration held constant at 2*M*.

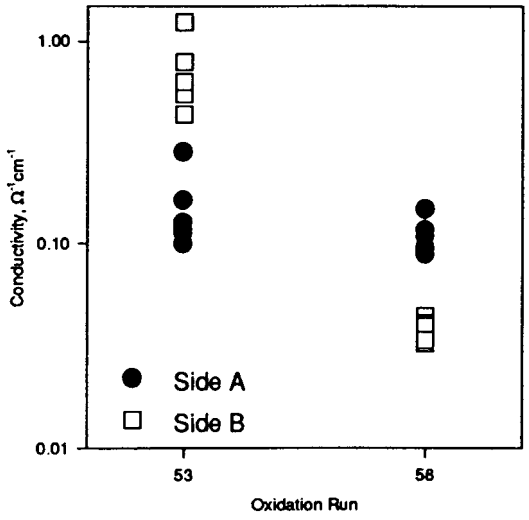

Figure 12 Plot of conductivity of random samples of films cut from runs 53 and 58 with contacts sputtered on side a or side b (arbitrary assignment).

concentration held constant at 2.0*M* is shown in Figure 10. For experimental temperatures up to 30°C, this surface is reasonably consistent with that for the original model shown in Figure 6. Conductivity falls off fairly rapidly over 40°C. Another view of the response surface is shown in Figure 11 with temperature held constant at the optimum value of 38°C.

To quantify the variation within single samples, 12 conductivity specimens were cut from each of two runs (53 and 58). Kapton films can have different surface functionality from side-to-side because of the manufacturing process.[20] For that reason, the sides on which the contacts were placed for conductivity measurement were carefully tracked. The conductivities from each sample and each side (*arbitrarily* assigned *A* and *B*) are plotted in Figure 12. The standard deviation in a single sample, using all the data points from a single run, was 0.22 $\log(\Omega^{-1}\ \mathrm{cm}^{-1})$. Two-way ANOVA showed that for each run a significant difference between the sides was detectable with greater than 95% confidence. Standard deviation across a sample decreased to 0.13 $\log(\Omega^{-1}\ \mathrm{cm}^{-1})$ when all measurements were taken from a single side. Hence, side-to-side variation accounts for a considerable amount of the total within-sample variation, but was not taken into account in analysis of the design data.

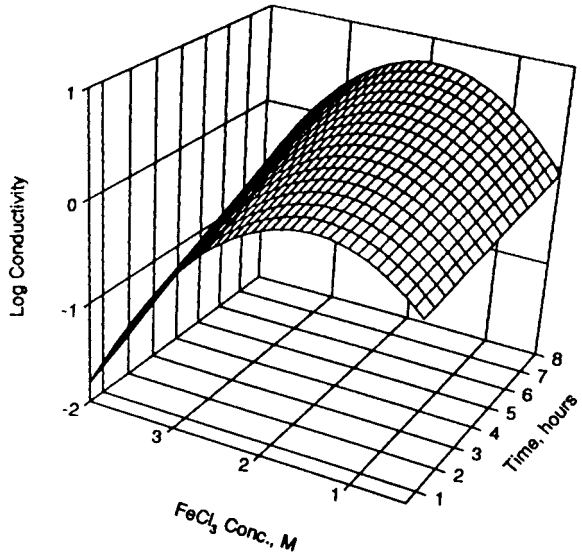

Figure 11 Response surface for *p*-3MT/Kapton with temperature held constant at 38°C.

Scanning electron microscopy (SEM) was performed on the surfaces, scalpel-cut cross sections, and liquid N_2 fracture surfaces of both treated and untreated Kapton. The surface morphology of the untreated Kapton is featureless below 15,000× magnification. Apart from fine parallel cut marks from the scalpel, micrographs of a cross section of untreated Kapton also revealed a homogeneous microstructure as shown in Figure 13(a).

Oxidized films had a quite different appearance as illustrated by micrographs of specimens produced in run 55 shown in Figure 13(b)–(d). The scalpel-cut cross-sectional backscatter image (BSE) shown in Figure 13(b) clearly reveals the depth of penetration of the oxidation layer. Comparison

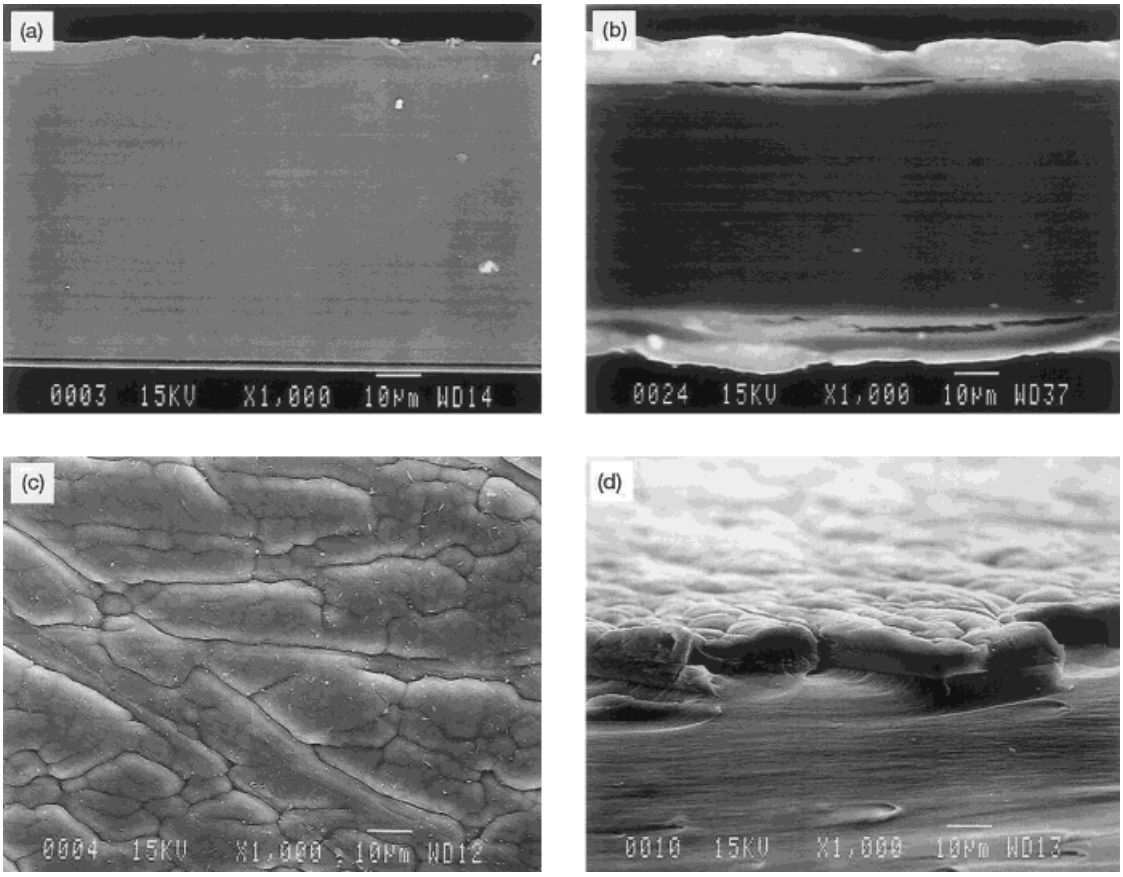

Figure 13 SEM of untreated Kapton and *p*-3MT/Kapton films from run 55: (a) BSE micrograph of scalpel cut cross section of untreated Kapton at 1000× magnification; (b) 1000× BSE micrograph of scalpel cut cross section of specimen from run 55; (c) SE surface of 55 at 1000× magnification; (d) SE image of liquid N_2 fracture surface at 1000× magnification and tilted at 15° angle.

of the total film thickness of the *p*-3MT/Kapton [Fig. 13(b)] with untreated Kapton at the same magnification [Fig. 13(a)] indicates that the conductive phase is incorporated into the polyimide rather than just coating the surface. The oxidation layer of films treated at less than optimum conditions are not as thick or distinct. Some debonding of the oxidation layer is also evident in Figure 13(b). While this may be the result of cutting the sample, it does suggest a weak interface. An irregular surface and fine microcrack development are characteristic of the surface of the treated films as shown in Figure 13(c) and (d).

The persistence of the conductivity over time of the films exposed to different environments was also investigated. For the Kapton/*p*-PY films, the conductivity tended to drop by about half an order of magnitude in the first several days at lab ambient conditions. After approximately 20 days, the conductivity stabilized to a value that did not change as much over the next 30 days. Conductivity of Kapton/*p*-3MT specimens exposed to air under ambient temperature was monitored for up to 300 days. Plots (log scale) of several different specimens are shown in Figure 14. The data points in each line are from a single specimen measured repeatedly over time. As shown, the decay in log conductivity followed a linear rate. After 300 days in air, the conductivity of the films dropped between a half to a full order of magnitude. This is typical of all the Kapton/*p*-3MT films made from all the different oxidant conditions.

Specimens cut from a film prepared under optimum conditions (run 56) were exposed to air at 100°C and the conductivities measured. The plot is shown in Figure 15. Since contacts sputtered on the samples for four-point measurements would not consistently survive exposure to 100°C, each point on the plot represents a different film specimen cut from run 56. Conductivity dropped

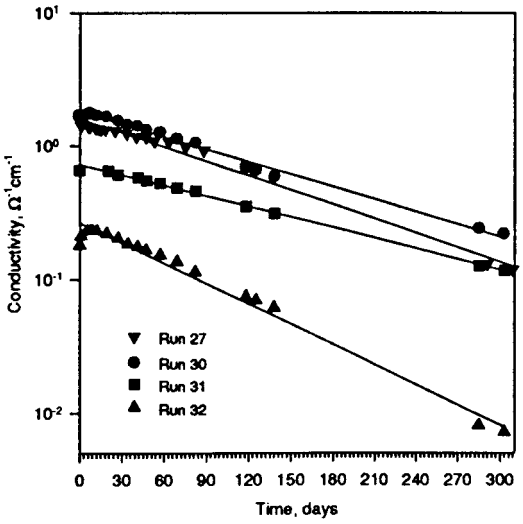

Figure 14 Plot of representative *p*-3MT/Kapton runs aged in air at room temperature.

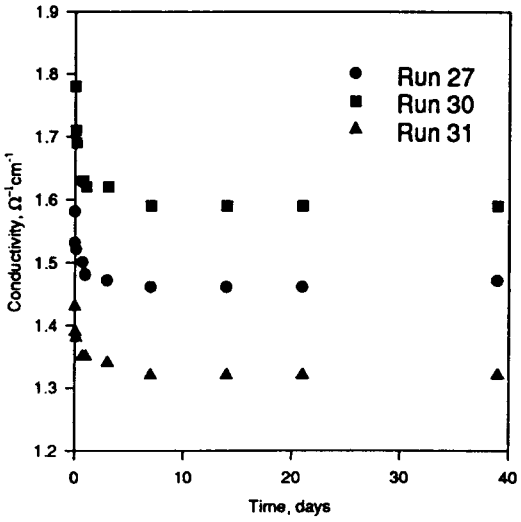

Figure 16 Plot of representative *p*-3MT/Kapton runs aged in a vacuum at room temperature.

off much more rapidly at this temperature. After only 120 h, the films dropped about four orders of magnitude in conductivity. The conductivity of specimens aged longer than 120 hours at 100°C could not be measured. The films were still uniformly dark in appearance.

The conductivity of films stored under vacuum at ambient temperature were also monitored for up to 40 days. The conductivity dropped only slightly on the first day, but did not change thereafter. Plots of representative samples are shown in Figure 16. This suggests that if the films are protected from air and perhaps moisture the conductivity will persist indefinitely.

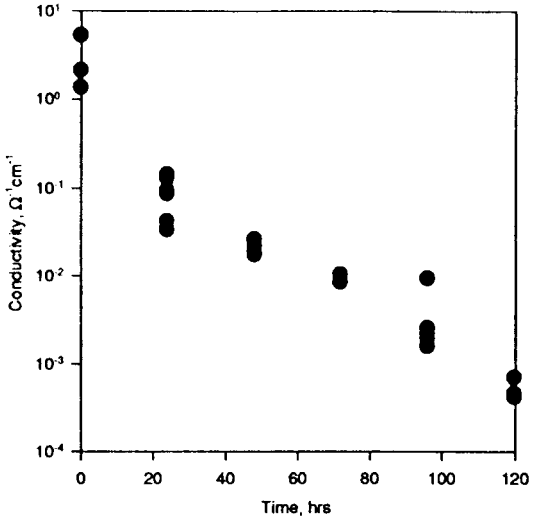

Figure 15 Plot of random samples cut from a *p*-3MT/Kapton prepared under optimum conditions and aged in air up to 120 h at 100°C.

CONCLUSIONS

A method to generate conductive film composed of small amounts of conductive polymer absorbed into the surface of polyimide films was optimized. Although tested on a small scale, this method should be easily scaled up to larger surfaces. Suitability of this method to the treatment of other surfaces, such as polymer matrix composites, is currently under investigation.

Both PY and 3MT were evaluated as precursors for the conductive phase of the composite films. Predictive models were empirically derived for each precursor to describe the effect of oxidation variables on the conductivity of the films. The oxidation variables studied were found to be highly interactive for both PY and 3MT. In other words, there was not a simple effect of time, temperature, or oxidant concentration on the conductivity. An optimum set of conditions was found for each conductive polymer to produce the highest conductivity.

Using *p*-3MT as the conductive phase, conditions were identified that produce films with conductivity as high as 5.7 Ω^{-1} cm^{-1}. The highest conductivity achieved with *p*-PY/Kapton was approximately two orders of magnitude less than the highest *p*-3MT/Kapton films. However, this

conductivity is still two orders of magnitude higher than previously reported results from other investigators using Kapton or another polyimide as base polymers. In fact, these values are more consistent with results using other base polymers with the same oxidation conditions, even when the base polymer was much more porous. Hence, the conductivity appears to be much more dependent on the conductive phase and oxidation conditions employed than on the base polymer chosen.

As evidenced from photomicrographs, films produced at less than optimum conditions contained less conductive polymer. Presumably, at more strenuous conditions, the conductive phase is simply overoxidized. Since PY is more easily oxidized than is 3MT, the conditions needed to produce optimum *p*-3MT-containing films were more vigorous than those sufficient to produce optimum *p*-PY-containing films.

Mechanical properties of the *p*-3MT/Kapton films treated at optimum oxidation conditions are only marginally significantly lower than that for untreated Kapton. If better mechanical properties are needed, compromise conditions can be chosen from the response surface models that give slightly lower conductivities. The conductivities of *p*-3MT/Kapton films tested over time under ambient temperature in air persist fairly well for 300 days. Vacuum-aged samples dropped only slightly in the first day and did not change thereafter.

REFERENCES

1. C. Li and Z. Song, *Syn. Met.,* **40,** 23 (1991).
2. D. Stanke, M. L. Hallensleben, and L. Toppare, *Syn. Met.,* **55–57,** 1108 (1993).
3. M. Morita, I. Hashida, and M. Nishimura, *J. Appl. Polym. Sci.,* **36,** 1639 (1988).
4. H. Van Duk, O. Aagaard, and R. Schellekens, *Syn. Met.,* **55–57,** 1085 (1993).
5. E. Ruckenstein and J. S. Park, *J. Electron. Mater.,* **21**(2), 205 (1992); E. Ruckenstein and J. S. Park, *Syn. Met.,* **44,** 293 (1991); E. Ruckenstein and J. H. Chen, *J. Appl. Polym. Sci.,* **43,** 1209 (1991).
6. E. Ruckenstein and J. S. Park, *Polym. Compos.,* **12**(4), 289 (1991); E. Ruckenstein and J. S. Park, *J. Appl. Polym. Sci.,* **42,** 925 (1991).
7. L. H. Dao, X. F. Zhong, A. Menikh, R. Paynter, and F. Martim, *Annu. Tech. Conf.-Soc., Plast. Eng.,* **49,** 783 (1991).
8. B. Tieke and W. Gabriel, *Polymer,* **31,** 20 (1990).
9. A. Angeli, *Gazz. Chim. Ital.,* **46,** 279 (1916).
10. For reviews, see T. A. Skotheim, Ed., *Handbook of Conducting Polymers,* Vols. 1 and 2, Marcel Dekker, New York, 1986.
11. S. Machida, S. Miyata, and A. Techagumpuch, *Syn. Met.,* **31,** 311 (1989).
12. J. B. Schlenoff, F. Yoke, and C. Shen, *Macromolecules,* **24,** 6791 (1991).
13. Y. E. Whang, J. H. Han, T. Motobe, T. Watanabe, and S. Miyata, *Syn. Met.,* **45,** 151 (1991).
14. K. Yoshino, S. Nakajima, S. Fujii, and R. Sugimoto, *Polym. Commun.,* **28,** 309 (1987); J. R. Reynolds, J. P. Ruiz, A. D. Child, K. Nayak, and D. S. Marynick, *Macromolecules,* **24,** 678 (1991).
15. M. A. B. Meador, J. R. Gaier, B. S. Good, G. R. Sharp, and M. A. Meador, *Sampe Q.,* 23 (1990).
16. E.g., see S. Hotta, S. D. Rughooputh, and A. J. Heeger, *Syn. Met.,* **22,** 79 (1987); Y. Wang and M. F. Rubner, *Macromolecules,* **25,** 3284 (1992); M. Raghu, C. O. Yoon, C. Y. Yang, D. Moses, and A. J. Heeger, *Macromolecules,* **26,** 7245 (1993).
17. J. E. Osterholm, P. Passiniemi, H. Isotalo, and H. Stubb, *Syn. Met.,* **18,** 213 (1987).
18. L.-C. Hsa, PhD Dissertation, University of Akron, 1991, p. 54.
19. J. Laakso, H. Jarvinen, and B. Skagerberg, *Syn. Met.,* **55–57,** 1204 (1993).
20. M. K. Williams, M. Huelskamp, J. Brandon, and M. Fisher, in *Proceedings of the 4th International SAMPE Electronics Conference,* June 12–14, 1990, p. 407.